



rijksuniversiteit  
groningen

faculteit wiskunde en  
natuurwetenschappen

# Solidification of Gallium films

Author: Paul Vermeulen

July 12, 2012

Supervision: Prof. Bart Kooi  
Second Supervisor: Dr. George Palasantzas

## Abstract

This research project focused on the solidification of Gallium films. The project consisted of two major parts: The first was the design of an experimental setup that was capable of freezing a Gallium layer by undercooling it, and capture and analyze the growth rate of Gallium crystals. An experimental setup was successfully designed that could induce controlled growth of Gallium crystals from a cold source. The growth speed of these crystals was analyzed using a camera and a Matlab image processing script. A thermocouple was used to investigate the temperature gradients applied across the layer. In the second part, several measurements were performed with this setup. The growth rate of these Gallium crystals was proven to be controllable by varying the layer thickness and level of undercooling applied to the layer. From our measurements we conclude that an increased temperature gradient across a Gallium layer increases the crystal growth rate in this layer.

# Contents

<b>1</b>	<b>Introduction</b>	<b>4</b>
<b>2</b>	<b>Theory</b>	<b>5</b>
2.1	Phase-Change materials . . . . .	5
2.1.1	Crystal Nucleation . . . . .	6
2.1.2	Motivation . . . . .	6
2.1.3	Temperature dependent growth . . . . .	7
2.1.4	Explore a different transition . . . . .	8
2.2	Heat Transport . . . . .	9
2.2.1	Steady state temperature gradients . . . . .	9
2.2.2	Heat and cold source connection . . . . .	9
2.2.3	Non-steady state. . . . .	10
2.2.4	A changing temperature gradient . . . . .	10
2.2.5	Influencing undercooling . . . . .	10
2.2.6	Summarizing heat conduction . . . . .	11
2.3	Crystal structure of Gallium . . . . .	13
<b>3</b>	<b>Building the experimental setup</b>	<b>14</b>
3.1	The first iteration . . . . .	14
3.2	Using a better cold bath . . . . .	16
3.3	Replacing water with Gallium . . . . .	17
3.3.1	Gallium-oxide . . . . .	17
3.3.2	Adding a thermocouple on the tray . . . . .	18
3.4	The final experimental setup . . . . .	19
3.5	The sample trays . . . . .	20
<b>4</b>	<b>Data acquisition and analysis</b>	<b>22</b>
4.1	An automated measurement . . . . .	22
4.2	Image processing in Matlab . . . . .	23
4.2.1	Subtracting two images . . . . .	23
4.2.2	From boundary timestamps to one growth speed . . . . .	24
4.3	Measuring temperature gradients . . . . .	25
4.4	Measuring crystal angles . . . . .	28
<b>5</b>	<b>Results</b>	<b>29</b>
5.1	Several early experiments . . . . .	29
5.1.1	Measuring crystal angles. . . . .	29
5.1.2	Crystal growth speed in an extremely thin layer. . . . .	30
5.2	Results from measurements with final experimental setup. . . . .	31
5.2.1	Crystal growth rate versus Nitrogen level for more trays. . . . .	32
5.2.2	Conclusions about crystal growth rate versus Nitrogen level . . . . .	33
5.2.3	Some speculation about other conclusions . . . . .	33
5.3	Investigation on temperature gradients . . . . .	34
5.3.1	Conclusions from temperature gradient analysis . . . . .	38
5.4	Temperature gradients versus crystal growth rate . . . . .	39

<b>6</b>	<b>Discussion</b>	<b>40</b>
6.1	Undercooling . . . . .	40
6.2	The tray-razorblade-heating plate-construction . . . . .	40
6.3	Thermocouples . . . . .	41
<b>7</b>	<b>Conclusions</b>	<b>42</b>
<b>8</b>	<b>Recommendations for further research</b>	<b>43</b>
8.1	Achieving higher undercooling . . . . .	43
<b>9</b>	<b>Acknowledgements</b>	<b>44</b>
<b>10</b>	<b>References</b>	<b>45</b>
	<b>Appendices</b>	<b>46</b>
<b>A</b>	<b>Custom Matlab code</b>	<b>46</b>

# 1 Introduction

In this report an account is given of the bachelor research project I did at the Nanostructured Materials and Interfaces group at the Rijksuniversiteit Groningen. This research project focused on the solidification of thin Gallium films. The project consisted of two major parts:

The first was the design of an experimental setup that was capable of freezing a Gallium layer by undercooling it, and capture the growth of Gallium crystals with a camera. For this several challenges had to be overcome, including quickly but controllably cooling a Gallium layer from one side, and finding a reliable way of recording and processing measurements of a growing Gallium crystal. In the design process, we started out with a basic design idea, and kept modifying and adding to the setup until we could reliably, and reproducibly grow Gallium crystals. After this first goal was accomplished, some measurements were performed.

The second part of this research project consisted of several measurements with the setup. These measurements focused on the effect of the amount of cooling and the effect of Gallium layer thickness, on the Gallium crystal growth rate.



## 2 Theory

This research project was explorative in nature, which means that when we started this project it was not completely clear what would be the most interesting measurement we could do. This was mainly a consequence of not having built the experimental setup, so it was still unknown what characteristic of freezing Gallium would be easily measurable. It was also unknown which variables would be easiest to vary. The research project was done in the context of other research conducted in the NMI (Nanostructured Materials and Interfaces) group on phase-change materials. Therefore we will first give a short introduction into this kind of materials, and their interesting properties.

### 2.1 Phase-Change materials

Phase change materials are a class of materials that can exist in two (or more) phases, within one state of matter. For instance GaSb and GeSb, the two materials on which NMI currently focuses, can exist in their solid state as either a crystalline or an amorphous phase as is displayed in figure 1. Here crystalline means an atomic roster, consisting of unit cells repeating in every direction, with a constant k-vector [4]. The amorphous structure still consists of the same atoms, but not in a repeating pattern, but such that there is no long-range order, but generally there is still a considerable amount of short-range order.

The research in NMI focuses on the transition between these two states, which can be induced by applying heat to crystallize the amorphous material (figure 1). Heating can be done in a furnace or on a hot plate, but for most applications local heating is required. This is done by using a laser focusing on a small spot, or by sending electrical currents through nanoscale wires made of a phase-change material.

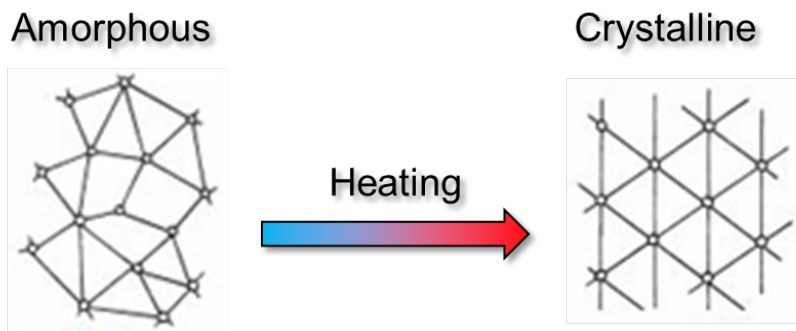


*Figure 1: Under influence of heat amorphous areas in a phase change-material can change to crystalline structures.*

This crystallization is obviously a temperature dependent phenomenon. If one would take a film of GaSb with a known Ga/Sb-ratio, and heat the whole film to a certain temperature, the crystal growth speed, the rate at which crystals grow is only dependent on this temperature. It is important for this research project to note that this film is at a certain temperature when the crystals start growing. This process happens in a steady state, or equilibrium situation, with-

out any significant heat gradients. The consequence is the crystals or crystalline regions appear at unpredictable times and places, due to the stochastic nature of the nucleation process. Still, when averaging over a sufficient large volume (or area in case of a thin film) the nucleation process still follow deterministic principles. In figure 2 a few stills are shown from a crystal growth measurement in a thin  $Ga_{78}Sb_{22}$  film, as performed by a master student of NMI. The images show a clear contrast between the original gray amorphous material and the much more reflective white crystalline areas.

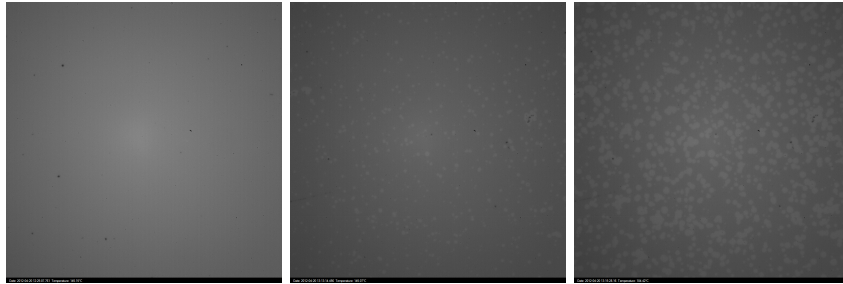


*Figure 2: Under influence of heat amorphous areas in  $Ga_{78}Sb_{22}$  change to a crystalline phase.*

### 2.1.1 Crystal Nucleation

The reason for the statistical nature of the crystal growth in figure 2 is that all crystals must start at a nucleation point, where the energy required to start crystal growth is relatively low. Once a crystal starts growing, the energy barrier to keep growing and adding more atoms to the lattice is lower than the initial nucleation-energy of a crystal [7]. Later on in the discussion of our results this point will be important.

### 2.1.2 Motivation

The reason of this interest in growth rates in phase change materials is their use in modern day society. Phase change materials can be used as data carriers, (i.e. cd's, dvd's bluray-disks, or other forms of data storage, see figure 3). Phase change materials are useful because the level of precision with which one can switch small areas within a material between crystalline- and amorphous states. These small areas can be used as bits, switching between 1 and 0 or amorphous and crystalline. These bits can either be read optically, by measuring reflectance, or by an electrical potential measurement. Because the amorphous phase has a higher resistivity than the crystalline phase. This contrast is essential for a phase-change to have practical applications.

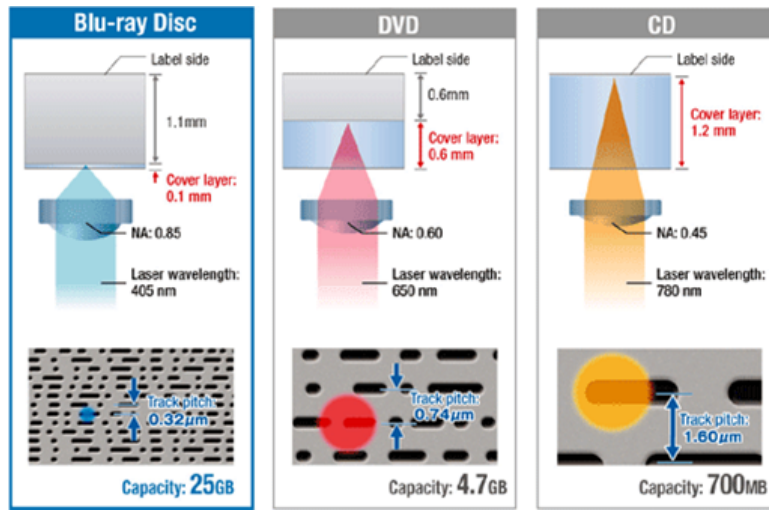


Figure 3: Several data carriers made of phase-change materials.

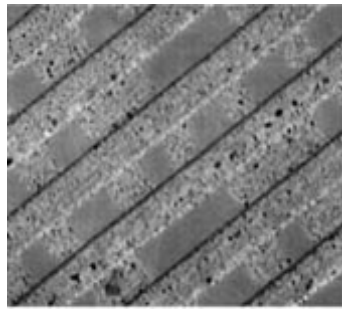


Figure 4: A data carrier needs to have optical contrast.

Most research focuses on either improving data carrier stability, ensuring the phase change material can change phase a lot of times without corrupting. The other main research topic concerns itself with increasing precision with which areas can be crystallized. In this way, the size of one bit can be reduced, allowing more data to be stored on one disk.

In both these areas, it is essential to know how fast and in what pattern crystals grow at certain temperatures in a phase change-material.

### 2.1.3 Temperature dependent growth

An important relation between crystal growth speed and temperature, that holds for a large number of phase change materials, is displayed in figure 5. This graph shows there will be no significant crystal growth at low temperatures, a drastic increase in growth rate for higher temperatures, then decrease as the material approaches its melting temperature. At the melting temperature there can be no crystals, since the material has completely liquefied. What this graph

describes is the same situation of heating that was mentioned above where the material is first heated to a certain temperature and then will start forming crystals, *at that temperature*. This can thus be thought of as a sort of steady state crystal growth.

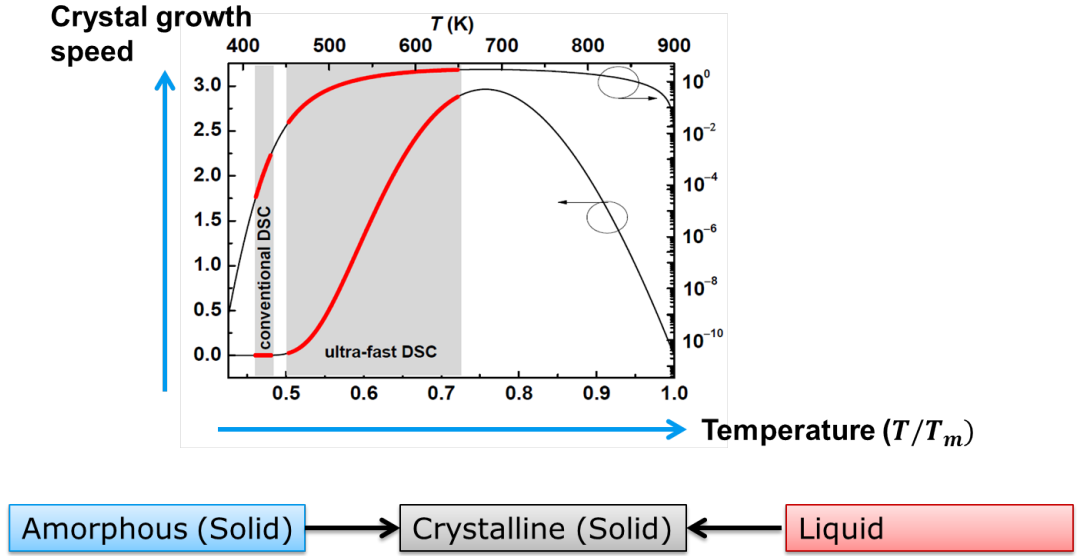


Figure 5: The graph shows crystal growth speed as a function of material temperature. The temperature is given as a fraction of the melting temperature, with all the way on the right the melting temperature ( $T_m$ ). Two lines are displayed, each with its own vertical scale. (Source: Orava, Greer et al. *Nature Materials* 11, 279283, march 2012)

#### 2.1.4 Explore a different transition

So far, the research from NMI has focused on crystallization in these amorphous solid films (i.e. the left slope of the graph displayed above). The aim of this research project was to investigate a different transition, specifically the transition from liquid to solid. The initial aim was to start off all the way to the right in figure 5, and cool a liquid Gallium film quickly to below the melting point. This should yield a layer of liquid Gallium below the freezing temperature. In this way, we hoped to reproduce the part of the slope on the right near the melting point. Here larger undercooling would mean an increased crystal growth rate, once the crystals started growing. It quickly turned out however, that the experimental setup in the form we built would not be able to induce large undercooling and most crystallization took place at, or just below, the freezing temperature. Gallium was chosen because it is a constituent of the GaSb films studied in the NMI group, and because the melting point of Gallium is at 29.76 °C. This temperature is thus very convenient for repeated heating and cooling experiments, because the melting temperature is just above room temperature.

## 2.2 Heat Transport

This brings up the matter of heat transport. For the experimental setup we built, it was necessary to have some understanding of heat transport phenomena.

### 2.2.1 Steady state temperature gradients

In a steady state situation, a system will be in thermal equilibrium. This does not necessarily mean all parts of a system have the same temperature. A system in a steady state situation can consist of a heat and a cold source, combined with a multi-material-connection. This system can then contain a steady state temperature gradient which depends on the materials between the two baths. The steepness of this gradient in a steady-state situation is dependent on a specific material property called thermal conductivity. The amount of energy transport per unit-time given a constant temperature gradient, measured in  $Wm^{-1}K^{-1}$  [5].

### 2.2.2 Heat and cold source connection

To repeatedly cool and heat the Gallium layers, an experimental setup that can both heat and cool these layers quickly is needed.

This means a connection is needed from the sample to a heat source (a heating plate) and a cold source (liquid Nitrogen). This connection should be made so that a large temperature gradient across the Gallium layer is created. This gradient is crucial, since it determines how much heat can flow away from the Gallium layer per second, thereby controlling the crystallization rate.

For the heating plate this is simple; the tray with Gallium is simply placed right on top of it. This insures no heat gradient will occur between heat source and sample; the sample temperature will match the heat bath temperature.

As a connection to the cold bath, we inserted a copper rod (copper conducts heat quite well ( $401 Wm^{-1}K^{-1}$  [2] ) in a duwar with liquid Nitrogen ( $-196^{\circ}C$  [3] ). This rod was isolated as much as possible to prevent air-copper contact. The other end of the rod was connected to the sample tray. In this way the temperature gradient from liquid Nitrogen to tray could be kept small, while still being able to have a large (practically infinite) cold bath. A schematic view of the experimental setup is shown below in figure 6, and will be discussed in more detail in section 3.4.

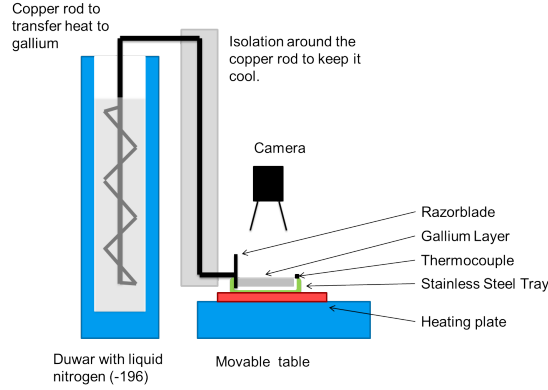


Figure 6: The experimental setup

### 2.2.3 Non-steady state.

Now there is a conduction path connecting the cold bath, our Gallium layer, and the heat source, it should be investigated what happens to the temperature profile of our system when an actual measurement is done. During a measurement temperatures will not be in their steady state-configuration.

The copper rod was soldered to a stainless steel razor blade, the same material as the tray containing our Gallium layer. This razor was placed in such a way it acted as one of the walls of the Gallium tray, in direct contact with our layer of Gallium. The razor acts as a cold surface from which crystal fronts can start growing out to the opposite side of our tray. This cold surface will be the first side of the tray to reach the solidification temperature of Ga ( $29.76^{\circ}\text{C}$ , [1]) after the tray has been heated. Therefore the first crystallization will start here, and slowly move toward the far end of the tray.

We assume the phase boundary, the edge between the solid and liquid Gallium, is exactly at the solidification temperature. This is a reasonable assumption since crystal growth speeds are quite low, and no undercooled Gallium will exist before crystallizing.

### 2.2.4 A changing temperature gradient

Once the heating plate is turned off the whole system will cool down to the temperature of the cold bath (neglecting air contact). The temperature gradient in the system will become smaller in time, flattening out to zero once the tray and Gallium reach liquid Nitrogen temperatures. This flattening will not be noticeable in the measurement range ( $60^{\circ}\text{C}$  to  $25^{\circ}\text{C}$ ) as the difference between a  $221^{\circ}\text{C}$  gradient and  $254^{\circ}\text{C}$  gradient is only roughly 10%.

### 2.2.5 Influencing undercooling

Because of the non-negligible length of the copper rod, the end connected to the razor will have a steady state temperature dependent on the length of this connection rod (i.e. the length not submerged in liquid Nitrogen). This means

that for a smaller length of the non-submerged part of the copper rod, the razor temperature will be lower, and it will cool down to that temperature quicker.

When the heating is switched off, the end of the rod and the connected razor falls to that (length dependent) temperature. The back end of the tray, away from the razor will follow. However, between the razor-side and far side of the Gallium layer, there will a temperature gradient. The steepness of this gradient depends on the speed with which the razor is cooled, which in turn is dependent on the length of the copper rod. These gradients, because the system is not in a steady state-situation, can be nonlinear. When the gradient is larger (a steeper slope), more Gallium can crystallize per second, since more energy can be conducted away from the Gallium per second. For this research we assume the gradient magnitude does not change too much during the crystallization process. This implies that the temperature distribution across the tray as a whole slowly moves down in temperature. This means that the melting point slowly moves in position away from the razor blade as the whole gradient moves down in temperature. This is sketched in figure 7. Essential for understanding the experimental setup and Figure 7 is that the experimental setup only uses one thermocouple that is at the far end of the Ga bath. So we know that the razor blade is at a lower temperature (although we do not know its temperature exactly), but we can record accurately the lowering of temperature as a function of time at the far end of the Ga bath. What we can conclude from this analysis is that we can influence the speed with which the crystal front moves forward by changing the speed with which the gradient drops.

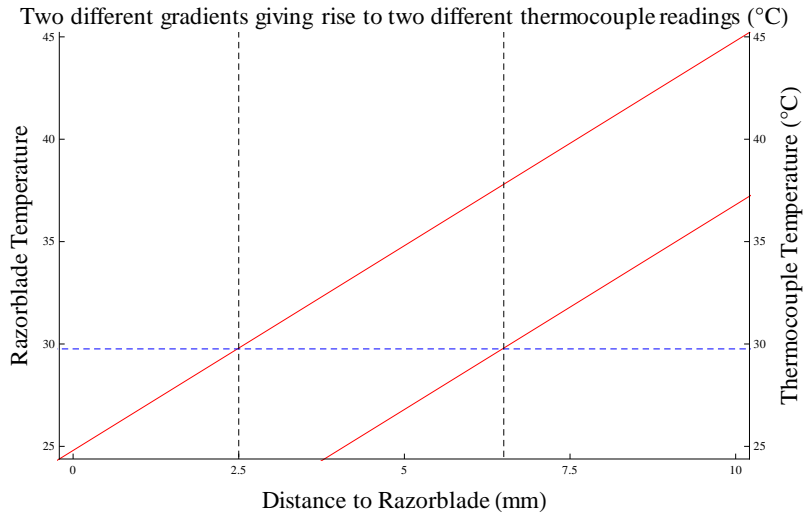


Figure 7: Moving the whole gradient (Red) down (in temperature) causes the crystal front to move forward (in position). The dashed crossings indicate melting temperature and front position.

### 2.2.6 Summarizing heat conduction

To freeze the Gallium, heat has to be conducted away from it, through the solid crystalline phase, the razor, and the copper rod, into the liquid Nitrogen.

Therefore, we can reason crystal growth is limited by several factors:

- The amount of Gallium (the layer thickness) to be solidified.
- The contact area between Gallium and the razor (through which all heat must to pass).
- The amount of heat that can be transported to the Nitrogen per unit of time (equivalent to length of non-submerged part of the copper rod or the *Nitrogen level*).
- The heat in the tray itself, which has to be removed too.

The most easily varied parameters are the amount of Gallium to be solidified, and the length of the copper rod not submerged in liquid Nitrogen. Therefore, these were the parameters we varied during our measurements.



### 2.3 Crystal structure of Gallium

Gallium has a fairly complicated (orthorhombic) crystal structure (see figure 8), with three different lattice parameters (Space group: Cmca (number 64), Cell parameters: a: 451.97 pm, b: 766.33 pm, c: 452.6 pm,  $\alpha$ : 90.000°,  $\beta$ : 90.000°,  $\gamma$ : 90.000° [6]). Therefore a Gallium crystal can grow with many different crystallographic planes as potential growth front, so the angles between individual planar growth fronts can have a large number of values too. Since first results were not promising, no more research into these angles, preferential crystal growth planes or the actual lattice structure around defects was done. We still mention the results of the first experiment, so it is also briefly mentioned here.

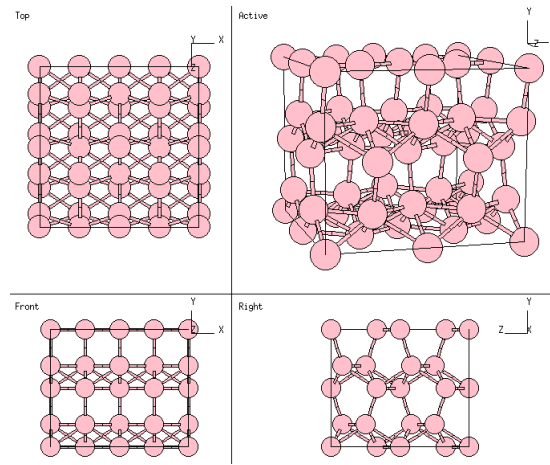


Figure 8: The crystal structure of Gallium, displayed from several angles. Source: <http://cst-www.nrl.navy.mil/lattice/struk/a11.html>.

### 3 Building the experimental setup

In this section first an account is given of the development of the experimental setup. In the final paragraph a full overview will be given of the experimental setup used to do the experiments of this research project.

#### 3.1 The first iteration

We started with the most basic system we could. A small aluminium tray (1 x 1 x 0.5cm) was made, with three slots (shown in figure 9). In these slots a stainless steel razor could be inserted, to divide the tray into two compartments (2.5mm deep), and provide a cold surface area. The tray was then placed below a high-speed camera. One of the two tray compartments was filled with water and liquid Nitrogen ( $-196\text{ }^{\circ}\text{C}$ ) was poured in the other. This setup was used to test if it was possible to induce freezing, and capture a growing crystal front of ice.

This experimental setup was sufficient to get used to the different processes that occur when cooling a sample before starting to use the more expensive Gallium. It was found that the razor, which was cooled by liquid Nitrogen could indeed conduct heat well enough into the water to create a crystalline front starting at the razor. The Nitrogen boiled away quite quickly however, so no constant temperature gradient could be applied across the tray, nor could the measurements be said to be sufficiently reproducible. Quite a lot of Nitrogen was used per measurement run (several tray compartments full). Several other cooling tactics were attempted, such as cooling down a copper rod in liquid Nitrogen and pressing it against the razor (figure 10), but this did not transfer enough heat to freeze the water. The camera was amply able to record the advancing crystal front, both in terms of framerate and lighting/contrast.

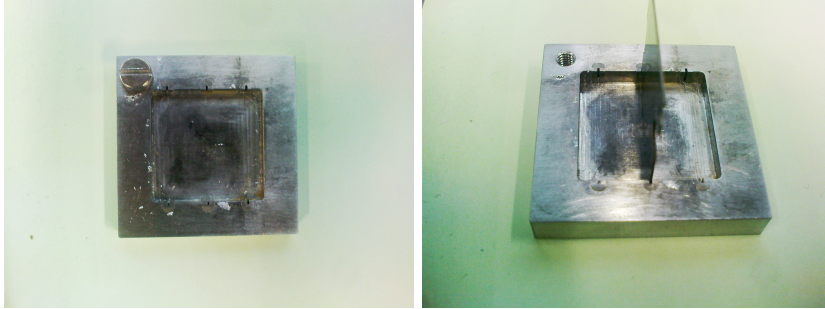


*Figure 9: Left: the aluminium tray (1 x 1 x 0.5 cm), with three slots for the razorblade. Right: The same tray, with a razorblade inserted in the middle slot.*

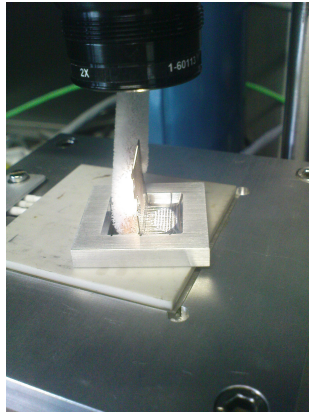


*Figure 10: A test design with the copper rod pressed against the razor.*

When analyzing the photos made of the freezing water, several issues became apparent:

- The water seemed to contain (and release upon freezing) large amounts of small air bubbles, as can be seen in figure 11. Although several sources suggested cooking the water to remove air, this did not work for us, probably because we had to put the water with a pipette into the small tray compartment, thereby letting air re-enter the water. Using de-mineralized water did not work either. We did not further analyse this problem because Gallium would not contain air.
- Although we always saw a clean freezing front in water, there also formed a layer of small rounded needle-like crystals (fig 12) on the bottom of the tray. It was found to be the bottom because a small pen was inserted in the water to check no surface ice was present.
- The image lighting would often flicker wildly, which was caused by clouds of Nitrogen gas streaming out of the duwar used to pour liquid Nitrogen on the other side of the razor.
- The freezing front speed was very much dependent on the amount of Nitrogen left in the compartment, as a refill would propel the front forward, lack of Nitrogen would cause the front to halt halfway through. In itself this was a positive result, as we could control the freezing speed. It also showed the experimental setup needed improvement so that the temperature of the razor as well as its capacity to absorb heat remained constant, meaning a much larger cold bath.

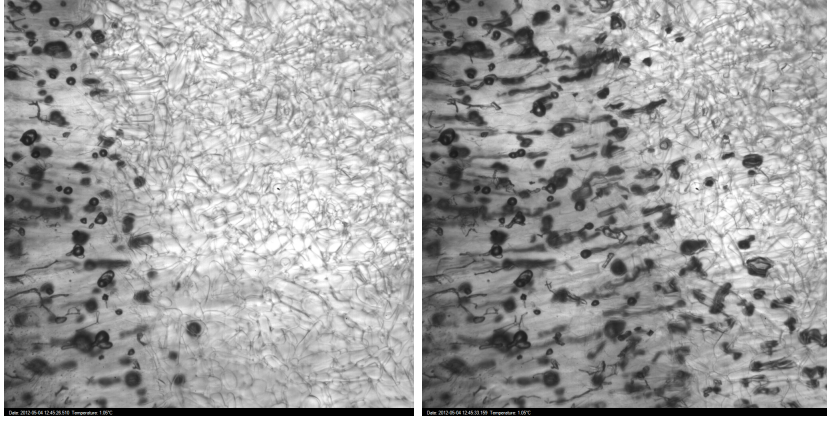


Figure 11: The freezing water front containing bubbles, where at the bottom of the water bath in an early stage already a thin layer of ice crystals is formed.

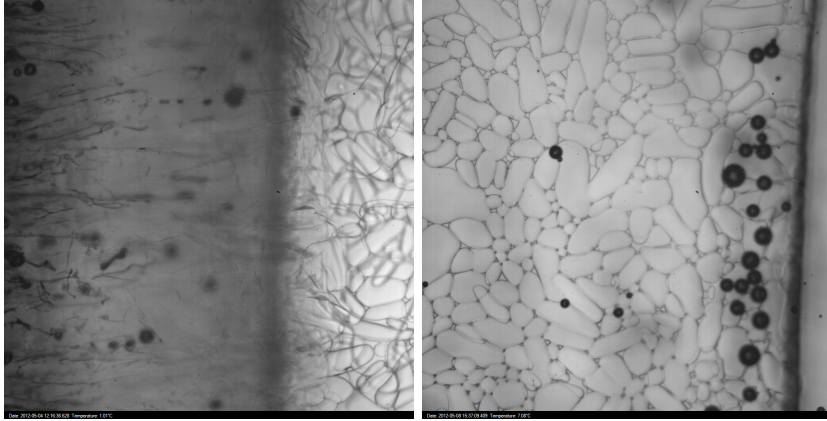


Figure 12: The bottom of the tray was apparently being cooled quickly, since small ice crystals formed there.

### 3.2 Using a better cold bath

The idea of pouring Nitrogen into a tray compartment was abandoned. In its place a copper rod (rounded, diameter  $\approx 0.5\text{cm}$ ) is soldered to the back of the razor. The rod was bent in shape so that it could be inserted into a duwar filled with liquid Nitrogen, yielding a much larger cold bath. However, this came at the price of having a larger conducting distance between cold bath and sample. The rod needed to be isolated with polystyrene foam to be able to cool the razor below  $30^\circ\text{C}$  within reasonable time. After the first measurement run with the copper rod a second rod was bent around the part submerged in Nitrogen to increase the contact surface between the rod and bath.

Using the copper rod and duwar gave a much more controllable cold bath, even though it does take a while for the copper rod to cool down and function

as an efficient cold source. After this setup produced some good and repeatable results, measurements were done using Gallium instead of water.

### 3.3 Replacing water with Gallium

The Aluminium tray was used for freezing water and after the first Gallium tests was replaced with a stainless steel one. This was done, because the Aluminium tray clearly degraded because of the Gallium, despite a protective aluminium-oxide-layer.

There were some more start-up problems with the Gallium. Since Gallium cannot be thrown away or removed as easily as water, it had to be possible to insert and remove the Gallium from the tray after the rest of the experimental setup was in place. This meant securing the tray to the razor blade with copper tape and later putting two razor blades in one tray slot to hold them in place.

Another challenge was getting the Gallium to spread out in the tray compartment to create a flat layer. Gallium wets very badly on almost any surface (we used glass, steel and aluminium all giving similarly large wetting angles). This meant the Gallium needed to be persuaded to change from its droplet shape to a nice flat layer in the tray. What seemed to work best was to put a large amount of Gallium in the tray, and then spread it out so it touched all edges of the tray and the razor. Next some Gallium was sucked away with a pipette. By using this technique, the Gallium would stick to all edges, and one could get the layer height to exactly that of the tray edges. Despite the fact this process yielded nicely flat layers, it limited measurements to completely filled trays.

Another trick to make this process easier was to heat the Gallium to at least 40°C (or for later experiments, 60°C), to lower its viscosity.

#### 3.3.1 Gallium-oxide

When preparing these layers, 'ripples' or 'blotches' could form on the surface of the Gallium. These are also visible on the recorded images (left image of figure 13), and would sometimes spontaneously appear with crystal growth and melting. Although we did not analyze the composition of these unwanted stripes, we expect them to be Gallium-oxide, formed from the contact with open air. A measurement was always started after these were removed by brushing a pipette very lightly over the layer, leaving a perfectly flat and highly reflecting Gallium-layer (right image of figure 13). Several measurement runs show these oxides appearing halfway through, but they seem to be of little influence to the crystal growth since they are only present in a very thin surface layer, and do not penetrate deeper into the layer.

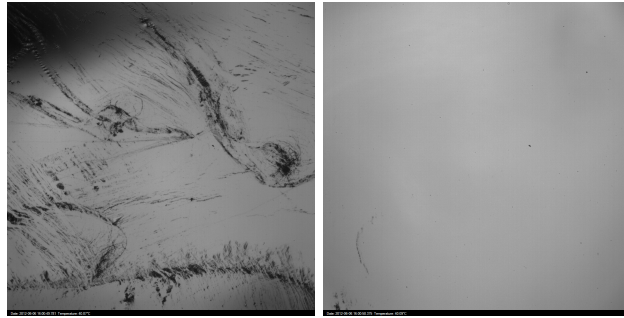


*Figure 13: On the left an image showing thin black lines we suspect are Gallium-oxide. These could be easily removed by wiping a pipette over the surface of the Gallium layer. A clean image made shortly after is shown on the right.*

### **3.3.2 Adding a thermocouple on the tray**

In a corner of the tray away from the razor (figure 14) a hole was drilled for a small thermocouple, held in place by a screw. This allowed us to measure the temperature of the tray at all times and even enable the control of the heating plate, e.g. keeping the tray at a certain temperature using a feedback system.

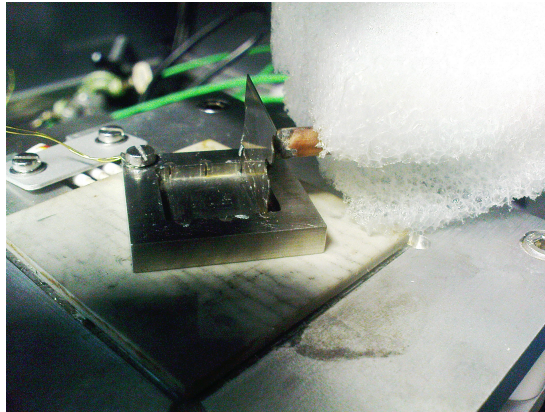


*Figure 14: The thermocouple is secured under the small screw.*

### 3.4 The final experimental setup

The final experimental setup is schematically shown in figure 15. A picture of the whole setup is shown in figure 16.

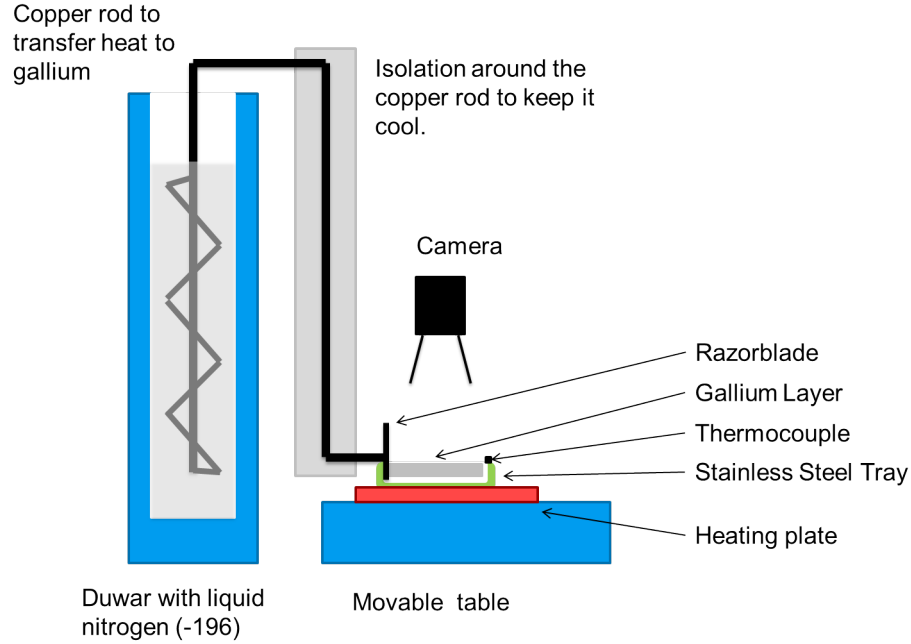


Figure 15: The experimental setup

In the middle of the image, on top the movable table (blue) and heating plate (red), the sample tray (green) is placed. The Gallium (gray) in this tray is bounded by the razor blade (black). On the back side of the razor blade a copper rod (black) is soldered (a close up can be seen in figure 14), with the other end fed into a duwar (blue) filled level with liquid Nitrogen (gray). The copper rod is isolated with polystyrene (gray). Temperature of the setup could be measured by two thermocouples; one in the heating plate below the tray, the other by the thermocouple on the tray side away from the razor (small black square).

Above the Gallium a photcamera (Photron 1024pci high speed CMOS camera) was suspended, making 1024x1024 pixel images every 0,5 second indefinitely, writing them to a harddisk immediately. Using a length calibration sample it was determined 160 pixels of a camera image spanned a length of 1 mm.





*Figure 16: The experimental setup*



### 3.5 The sample trays

For the Gallium tray several different samples were made, with the goal of varying both the Gallium layer thickness and the Gallium-steel contact area. These samples are shown schematically in figure 17. Every sample had the same dimensions, so the weight of the Gallium can be converted linearly to the depth of the tray left to the Gallium or the Gallium layer thickness. Another tray with a varying number of steel plates was used, to keep the contact between Gallium and tray (which was also made from stainless steel) the same, and vary the Gallium layer thickness. The solution of filling up the tray as opposed to having trays with different volumes was based on time constraint, having to wait for the fabrication of a new set of trays would take too long. The different isolation trays were used to determine how much heat flowed through the bottom of the tray, and how much passed directly from Gallium to the razorblade.

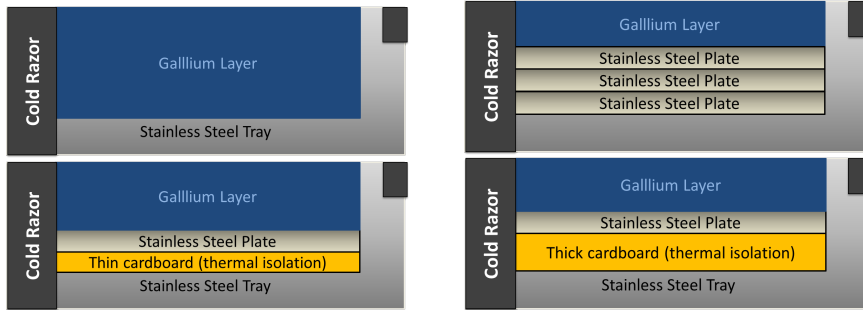


Figure 17: Schematic view of the different sample trays used. The actual trays used contained the following amounts of Gallium: 'only Gallium': 4.39 grams, 'thin isolation': 2.33 grams, 'three steel plates': 2.35 grams, 'thick isolation': 2.24 or 1.61 grams, 'two steel plates' (not depicted here): 3.06 grams.

## 4 Data acquisition and analysis

Now there is an experimental setup to do measurements on crystal growth speed, where we can vary a few parameters, such as the sample tray configuration and amount of undercooling (using the Nitrogen level in the duwar as a measure).

A typical measurement run, as possible at the very end of the research project, looked like this:

1. The razor, attached to the copper rod, is inserted in the tray slot far away from the thermocouple. Then the tray is filled with some steel plates and/or isolating cardboard.
2. The Gallium from a larger storage pot is heated using boiling water, then transferred to a smaller container from where it could be inserted and removed without contaminating the large supply.
3. Next the Gallium is put in the tray using a pipette. The easiest way was to put too large an amount in the tray and spread it out with the pipette, holding it parallel to the Gallium surface. Once the Gallium is no longer a droplet but a layer clinging to all sides (most importantly, the razor), the excess Gallium can be sucked away with the pipette. This step, where the Gallium layer/drops are manipulated, was much easier at higher ( $60^{\circ}\text{C}$ ) temperatures.
4. Next the previously mentioned Gallium-Oxides were removed to create a uniform surface.
5. Once the sample was completely prepared, liquid Nitrogen was poured into the duwar, to start the cooling process.
6. The first cooling was different from the rest, as the copper rod and razor still had to cool down from room temperature. Therefore we had to allow crystals to grow, then heat it again using the heating plate to a higher temperature above the melting temperature, melt the crystals again, and then start the real measurement.

### 4.1 An automated measurement

Once the measurement setup was prepared to actually measure, which took about half an hour, a computer programme was used to run a measurement of about three hours, in which the Gallium layer froze around 10-12 times before the Nitrogen in the duwar ran out. The computer programme contained a PID-control component that could regulate the tray temperature using the heating plate. A measurement schedule, specifying upper (far above melting temperature) and lower boundaries (after full crystallization) was entered in this control component before a measurement.

1. The thermocouple in the sample tray was used by the programme to measure the temperature. The sample tray was cooled down to below the freezing temperature ( $28^{\circ}\text{C}$ ). Causing a crystal to grow.
2. Once this temperature had been reached, the tray was heated to  $60^{\circ}\text{C}$  again, and kept there for two minutes to melt the crystal.

3. The heating plate is switched off, letting the sample cool down again.
4. Nitrogen level in the duwar was measured manually from time to time, using a ruler. By later combining this measurement to the timestamps of every camera image, we could interpolate what the Nitrogen level was for every crystal growth rate.

## 4.2 Image processing in Matlab

A Matlab script available in the NMI group was modified to measure growth speed of a large crystal front instead of the usual small crystal spots. The modified code can be found in appendix A.

### 4.2.1 Subtracting two images

The script relied on subtracting two images about five seconds apart (figure 18):

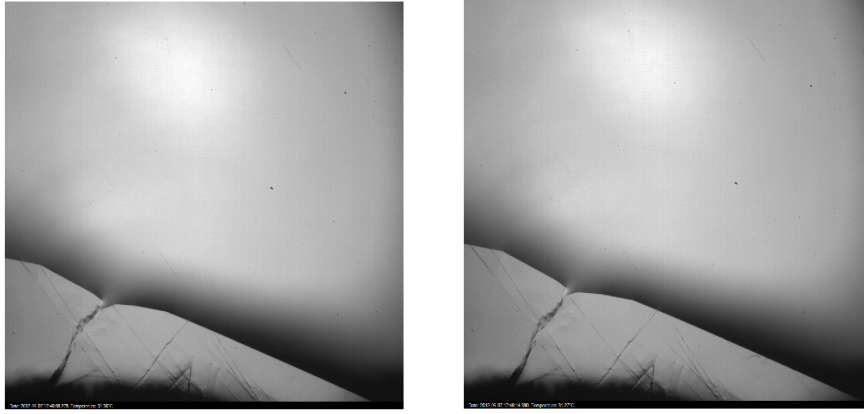


*Figure 18: The crystal front images we start with, right is some 10 frames later.*

These images are converted to grayscale, giving every pixel in the 1024x1024 images a value between 0 (black) and 1 (white). Then they are subtracted, causing all non-moving boundaries and features to disappear. Only where the crystal boundary had moved forward, the pixel values will be nonzero. Then Matlab's built-in edge detection function (Sobel-method) is used to detect the front and back edge of the crystal front (figure 19). This analysis is done for every frame of a measurement, always subtracting it from the image 10 frames later (5 seconds), yielding often around four-to five hundred binary images showing the edge of the crystal front. The script stores all timestamps belonging to the white pixels that makes up the edges, and overwrites them when a new edge passes. This is done so that only the timestamps of the back edge (which passes after the front edge), is recorded in the final image. In the end every pixel has a time stamp of when the back edge passed. Now the script can calculate growth speed for each point in the image, by looking at the movement speed of this back edge.

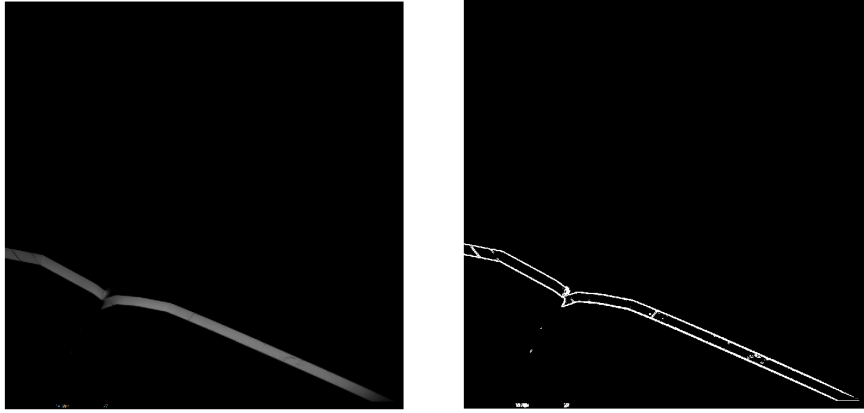


Figure 19: Two images subtracted (Left), after edge detection has been performed (Right)

#### 4.2.2 From boundary timestamps to one growth speed

All boundary images from a crystal growing in time are put into one image, by assigning to every pixel the time the crystal boundary passed there. Whiter pixels indicate a later time of passage of the front. Next a growth image is made, which averages in a circle of eight pixels the growth speed of that area by looking at the distribution of timestamps (figure 20). The data of these circles is then plotted in a histogram (figure 21). As can be seen, the data yields a peak at the most common growth rate. The width of this peak, the full width half max, is used as an errorbar for the measurement data obtained through this algorithm.

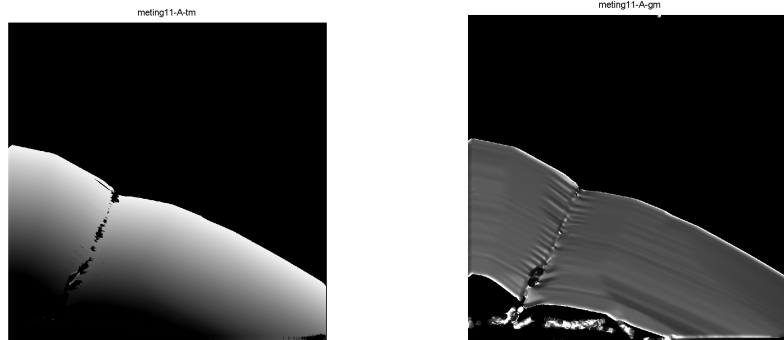


Figure 20: Left An image of the crystal front moving in time, where whiter pixels indicate a later time of passage of the crystal front. Right a growth image showing the growth speed (white indicates a faster growth speed).

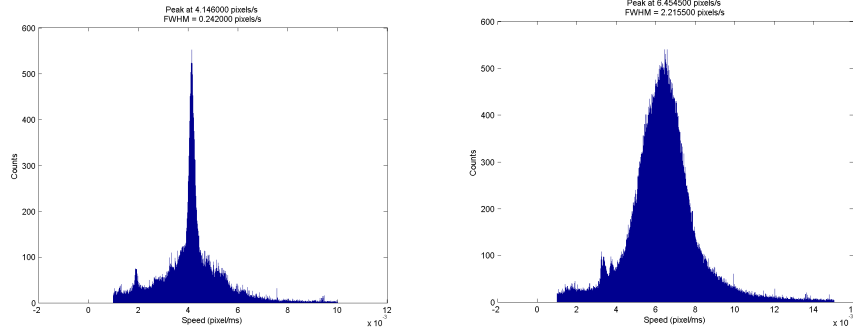


Figure 21: Two histograms resulting from the image analysis algorithm above.  $y$ -axis shows counts,  $x$ -axis displays growth rate. Every count is one data point from the growth image.

### 4.3 Measuring temperature gradients

When the first Nitrogen level versus crystal growth speed measurements were done, more information about the actual temperatures in the sample tray was needed. By recording the Nitrogen level, we could say the razor was cooled to a temperature that depended on this level, but not much more. By adding a thermocouple to the end of the tray, something could be said about the whole temperature gradient from liquid Nitrogen to thermocouple. Although a thermocouple on or near the razor would have been a much better position, this was impossible considering the current tray design. In figure 22 a top view of the tray is displayed, showing the locations of several key areas to our temperature gradient determination. The figure shows the sample tray (green), with Gallium layer (gray), crystal front edge (light gray), razor on the left (black), thermocouple on the right (black), and camera view on part of the Gallium layer (black dashed square).

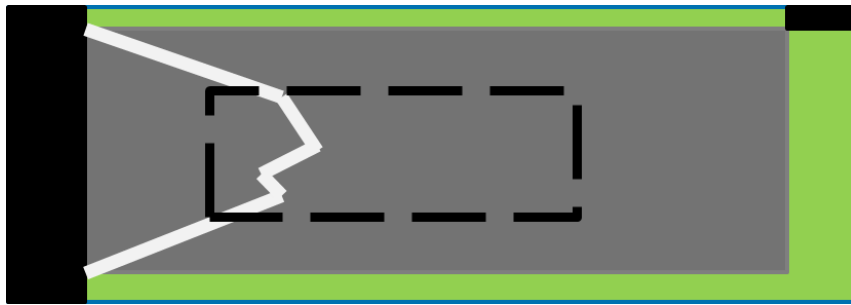


Figure 22: Top view of the sample tray (green), with Gallium layer (gray), crystal front edge (light gray), razor on the left (black), thermocouple on the right (black), and camera view of part of the Gallium layer (black dashed square).

The temperature of this thermocouple at two moments in time was measured; when a crystal front enters the camera view, and when it leaves the camera view again. An example crystal front is shown in figure 23.



Figure 23: The crystal front images when the crystal just enters the camera view (Left), and leaves it again(Right).

By analyzing the two temperatures with the help of figure 24 conclusions can be drawn about the magnitude of the temperature gradients in our tray.

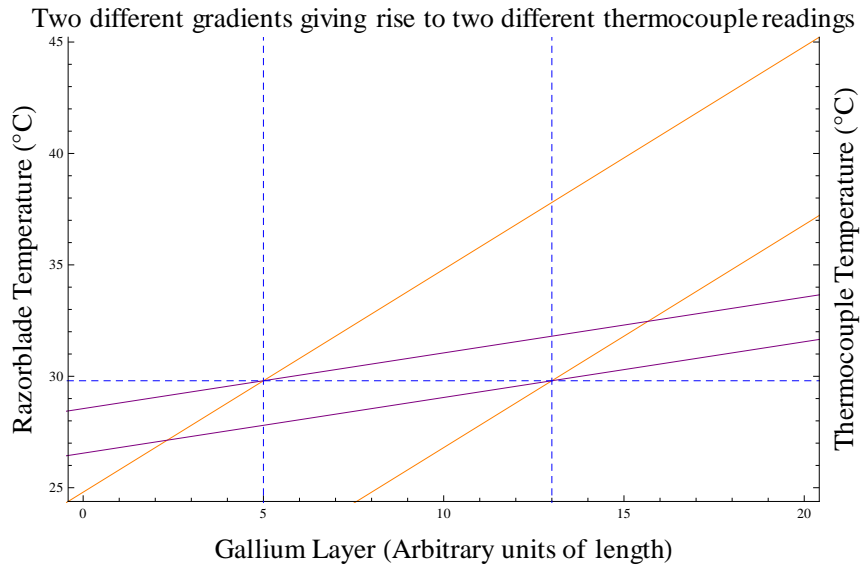


Figure 24: Two different gradients give rise to two different thermocouple readings. The high- and low- temperature difference is bigger, as are the absolute values of these temperatures, when the gradients are sharper. Temperature axes are in  $^{\circ}\text{C}$ , Gallium layer (position) axis is in arbitrary units of length.

Figure 24 shows two different gradients; a relatively steep one (Orange) and a much flatter one (Purple). The dashed lines represent the points in place and temperature where the crystal enters and leaves the camera view. Because of the low crystal growth speed observed, the crystal fronts were assumed to be at exactly the freezing temperature of Gallium ( $29.76^{\circ}\text{C}$ ).

On the left temperature axis the razor temperature is shown, on the right

axis the thermocouple temperature. The two are spatially separated by the Gallium layer (x-axis), through which the temperature gradient is a rising line we assume here to be linear. The linearity is not crucial for this analysis, as long as the gradients do not exhibit too sharp curves, they can have much more complex forms and the analysis would still hold. It is also assumed there are no large effects from the Gallium layer existing in two phases. The assumption that the different Gallium phases do not influence the gradient too much is justified because their heat capacities are of the same order of magnitude: 25,86 Jmol<sup>-1</sup>K<sup>-1</sup> and 31,56 Jmol<sup>-1</sup>K<sup>-1</sup> [1].

If first the steep gradient (orange) is examined, one can see it is caused by a lower razor temperature, whereas when the crystal just enters the camera view (start-temperature), a high temperature is recorded by the thermocouple. When the crystal front leaves the camera view (end-temperature), the temperature on the razor is still quite high, but there has also been a large decrease in thermocouple temperature.

If we examine the smaller temperature gradient (Purple), we see both crystal entering and leaving takes place at lower temperature readings of the thermocouple. The temperature difference between those two is much smaller than for the steeper gradient (orange).

Using this analysis, we argue that higher start-temperature (when crystal enters the camera view) and end-temperature (when the crystal leaves the camera view), as well as a larger difference between the two, mean a larger temperature gradient.

#### 4.4 Measuring crystal angles

As a short side-experiment, it was noticed during the preliminary crystal growths that the crystals grew with clearly distinguishable angles between different faces of the crystal. Since we hypothesized there might be preferred growth directions in the crystal lattice, an image processing programme called ImageJ was used to measure crystal angles by manually selecting crystal angles.

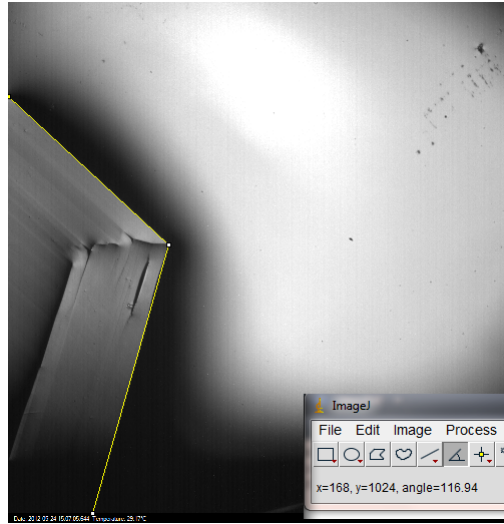


*Figure 25: Measurement of a crystal angle in ImageJ. the bottom right window shows the angle between the two crystal faces outlined with the yellow line.*



## 5 Results

### 5.1 Several early experiments

First the short accounts are given of two experiments that did produce a result worth mentioning but did not merit any further research.

#### 5.1.1 Measuring crystal angles.

While developing the setup, trying different techniques and studying the way crystals grow many different crystal formations were observed. For every individual crystal angle with large enough crystal faces the angle between these faces was determined. It was hypothesized that the crystal structure of Gallium might reveal itself through certain angles (and their multiples) showing up repeatedly. As can be seen in figure 27, no clear distinction was found, either because the crystal growth is too chaotic, or the sample size is simply too small to see statistically relevant bands or peaks appear. An issue which led to this small sample size was that often a crystal front does not form any distinct faces, as seen in the right image of figure 26.

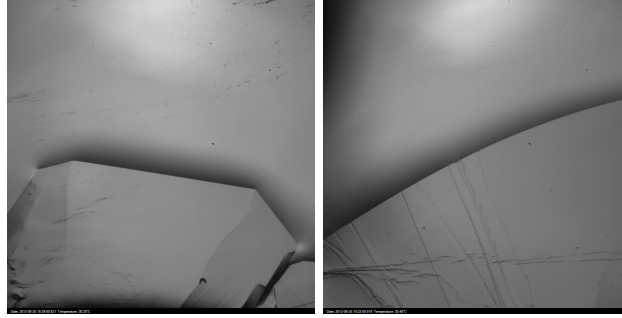


Figure 26: Two different crystal fronts, where the one on the left shows clearly distinguishable crystal faces, and the one on the right does not.

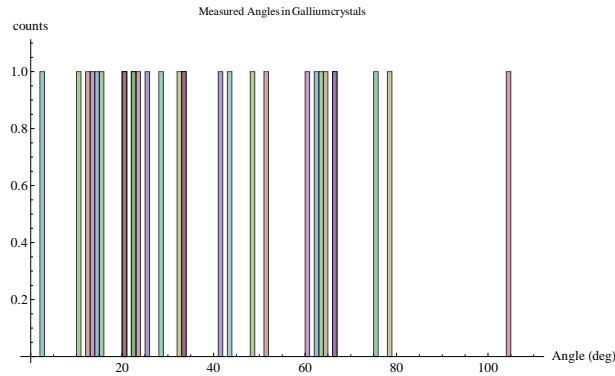
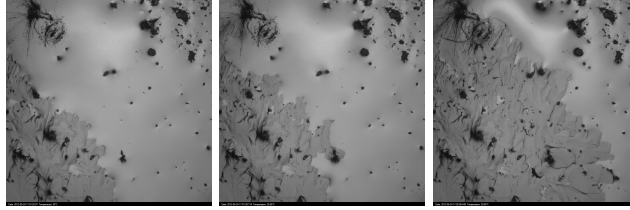


Figure 27: Histogram showing the distribution of crystal angles in the observed crystals.

### 5.1.2 Crystal growth speed in an extremely thin layer.

Another small experiment was done after a measurement on the tray with only Gallium. Afterwards, all Gallium was sucked away with a pipette, but for a thin layer  $\approx 0.5\text{mm}$  that clung to the bottom and edges. This layer contained holes and was not flat, but still connected to the razor, so it could still be cooled down again. This resulted in the images below (figure 28):



*Figure 28: In a very thin Gallium layer,  $\approx 0.5\text{mm}$ , crystal growth is much faster (these images are 30s apart). The crystals are also much smaller. The black spots are not oxide but holes in the layer)*

Even though this was very interesting, as apparently very thin layers crystallize very quickly, analyzing this kind of crystal growth proved difficult because of all the imperfections in the layer. Another issue was reproducibility, the layer was created by sucking away most Gallium, but there is no precise way to control layer thickness. For that reason, layers of this kind of thicknesses were not researched in greater detail.

## 5.2 Results from measurements with final experimental setup.

The first measurement was done with a sample tray with just Gallium (figure 17, 4.39 grams). This measurement was the last one where heating was done by hand and Nitrogen level was manually set to a certain level instead of allowed to decay in time. This measurement was done by first heating the sample to 40 °C, and keeping it at that temperature, then cooling it down until the sample was fully crystallized, and finally heated again. After this measurement was done it was decided to automate the measurement process further (as described in section 4.1), as this manner of data acquisition was very time-consuming.

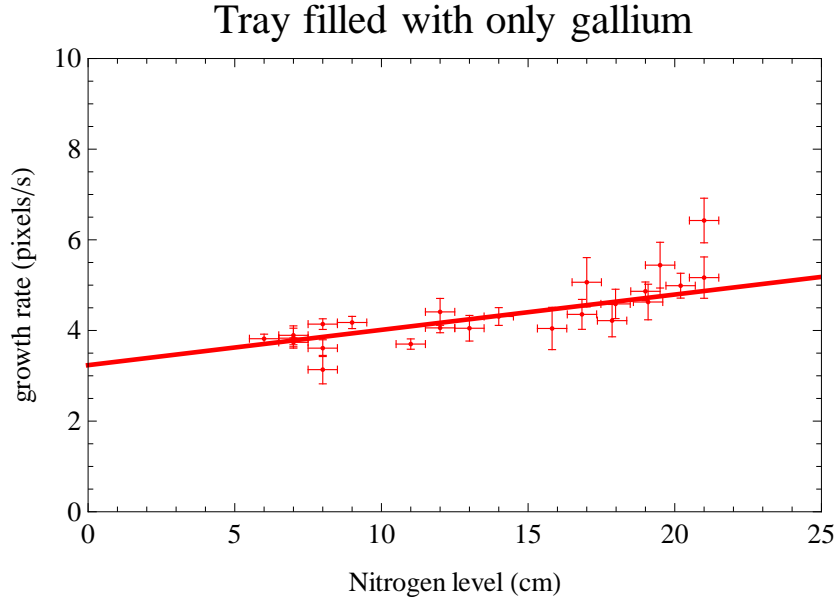


Figure 29: Tray with only Gallium, Nitrogen level versus growth rate.

The errors for each data point in this graph are chosen as  $\pm \frac{\text{FWHM}}{2}$ , where FWHM is the *Full Width Half Maximum* of the histogram (figure 21) of the growth rate of the specific crystal.

Through this dataset a linear fit is plotted, which takes into account the size of the individual errors. We can see a clear dependence of crystal growth rate on Nitrogen level. This measurement was reason to continue performing this kind of measurement on other sample trays (as depicted in figure 17). The data of this measurement will not be used because of the different way in which it was acquired, compared to the more consistent automated way of later measurements. Furthermore, in this measurement the sample tray was only heated to 40 °C, whereas the next set of measurements was done with tray heating to 60 °C, because close examination revealed that at 40 °C at the thermocouple a Gallium crystal still was present near the razor.

### 5.2.1 Crystal growth rate versus Nitrogen level for more trays.

A growth rate versus Nitrogen level measurement was performed for four sample trays; 'filled with three steel plates', 'filled with two steel plates', 'thin cardboard isolation', 'thick cardboard isolation' (figure 17). The results can be found below in figure 30.

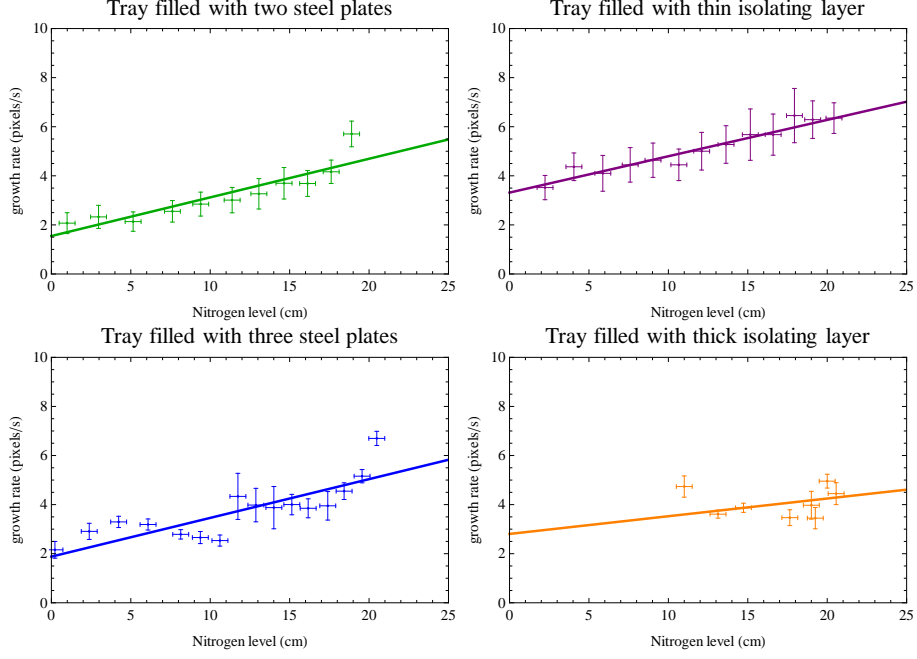


Figure 30: Growth rate versus Nitrogen level for differently filled trays.

Several conclusions can be drawn from these trends. The automated 'hands-off' measurement technique still yields a large scatter, but by performing a large amount of measurements, we can still see the same pattern emerging as for the tray containing only Gallium.

The measurement data set for 'thick isolation' is much smaller because the the crystal growth there became so messy at low Nitrogen levels that no growth rate analysis could be completed in Matlab.

The dataset for 'three steel plates' shows some non-linear trends, most notably a sudden discontinuity at  $\approx 12$  cm Nitrogen. Nonetheless, a linear fit still yields a relation remarkably similar to the 'two steel plates' and 'thin isolation', as shown in figure 31.

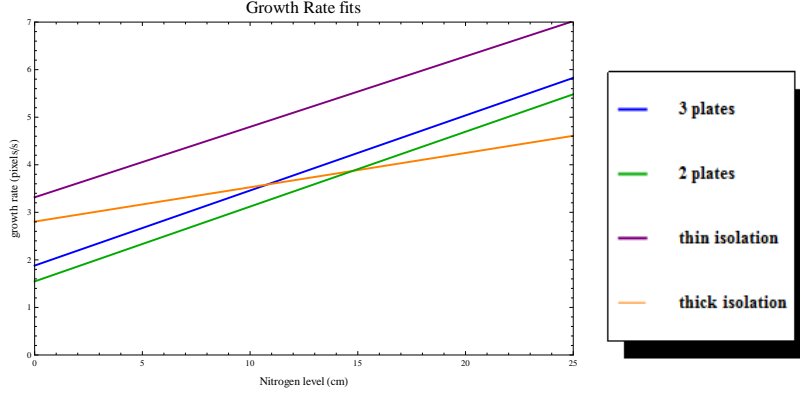


Figure 31: Growth rate versus Nitrogen level, fitted lines plotted for four differently filled trays. Layer weights (linearly translatable to thicknesses: 'thin isolation': 2.33 grams, 'three steel plates': 2.35 grams, 'thick isolation': 2.24 grams, 'two steel plates': 3.06 grams).

### 5.2.2 Conclusions about crystal growth rate versus Nitrogen level

In figure 31 the fits displayed in figure 30 are combined in one plot for comparison. The measurement series 'two steel plates', 'three steel plates' and 'thin isolation' show nearly identical relations between growth rate and Nitrogen level. Also the 'thick isolation' dataset shows an increase in growth rate for increased Nitrogen levels. Supposedly, the discrepancy between this tray and the other is caused by the smaller number of data points available to fit. Using this setup, Gallium crystal growth rate was observed to increase by approximately 3 pixel/s (equivalent to  $19\mu\text{m/s}$ ) when the Nitrogen level was increased from 5 cm to 20 cm. Therefore it can be concluded that an increasing Nitrogen level increases the crystal growth rate.

### 5.2.3 Some speculation about other conclusions

One can speculate about a few other conclusions that might be drawn from these measurements. The 'two steel plates' and 'three steel plates' show remarkably similar growth rates, even though the 'two plates' contained a Gallium layer that was about 30% thicker. This might mean layer thickness is not a significant factor when studying growth rates (at these layer thicknesses).

We do see that the 'thin isolation' growth speeds are higher than those of 'three plates' even though layer thickness is almost the same. We might conclude from this that by removing the thermal contact between Gallium layer and tray floor, the growth speed increases. However, this is immediately contradicted by the 'thick isolation' data, that exhibits lower growth rates at approximately the same layer thickness (thin isolation: 2.33 vs thick isolation: 2.24 grams). Even though it might be tempting to exclude this dataset from our analysis completely since the fit was based on a much smaller data set, see fig 30, that would leave us with only three samples, which in this case is not very much to base conclusions on.

The speculations above are no conclusions from our measurements, since we

do not have enough data, and also contradicting evidence on some conclusions. Nevertheless, they are useful as guides for further research.

### **5.3 Investigation on temperature gradients**

Because more knowledge was needed about how well our system is able to cool the Gallium layer, a thermocouple was added on the tray edge opposing the razor (see figure 22). Although in hindsight it should have been installed next to the razor, since this is a much more direct way to determine the amount of undercooling and the magnitude of the temperature gradient the razor blade could provide to the Gallium. Nevertheless, with the configuration and method of analysis explained in section 4.3 conclusions can be drawn about the magnitude of the temperature gradient as a function of Nitrogen level. In figure 32 the results of the temperature gradient analysis as described in section 4.3 are displayed, for the same trays as used before, with one change: 'thick isolation' now has a much thinner Gallium layer (1.61 grams).

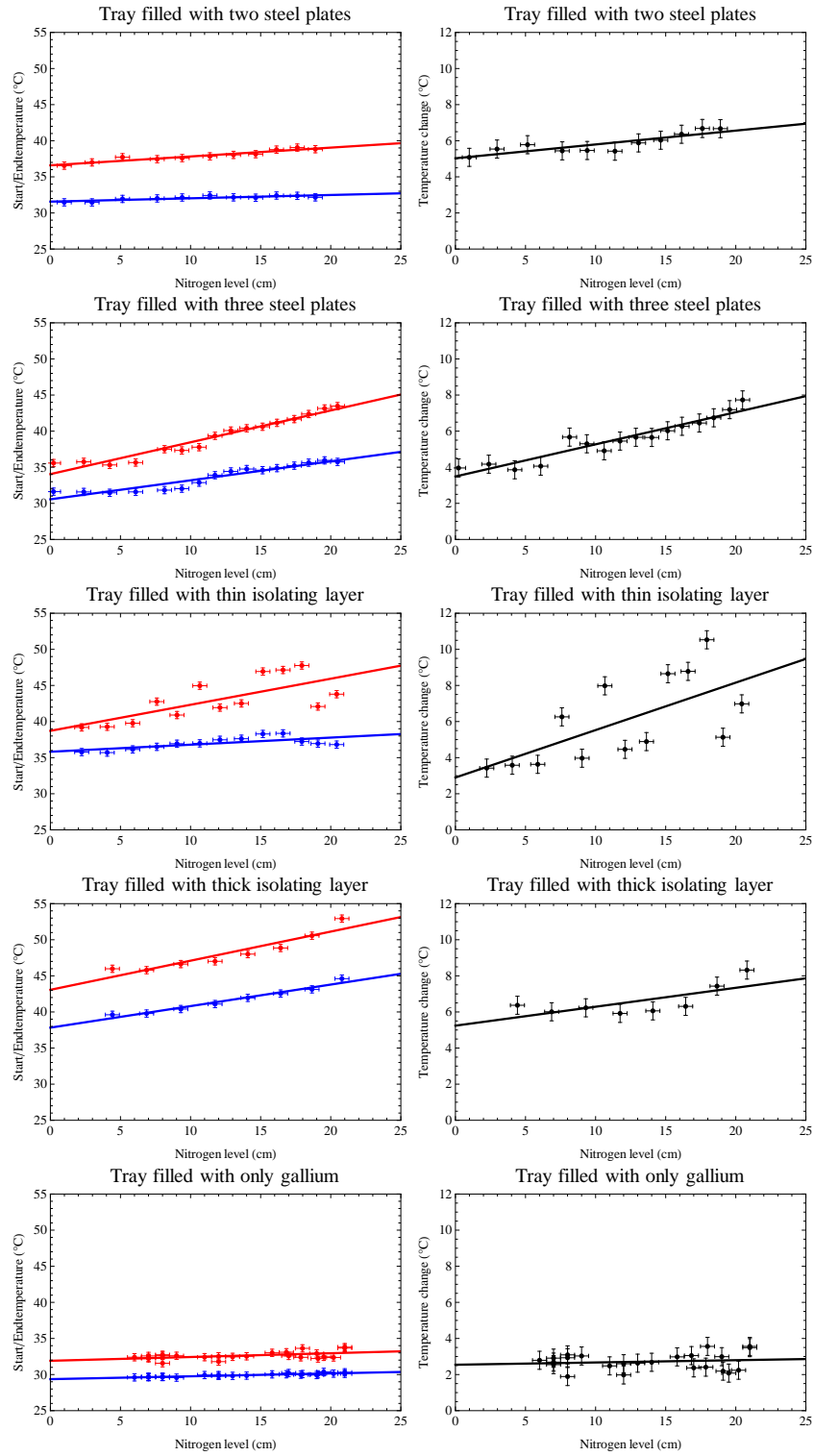


Figure 32: On the left the start-temperature (Red), and the end-temperature (Blue) as a function of Nitrogen level. On the right the temperature change, (start minus end) in black as a function of Nitrogen level.

A few overall trends can be observed. All data sets show an increase of start-temperature, end-temperature and change (start-temperature minus end-temperature) in temperature for higher Nitrogen levels. In most cases, start- and end- camera frames could be determined quite accurately. It is unclear what the reason is for the much larger scatter in the 'thin isolation' dataset. The much lower dependence of the 'only Gallium' tray on Nitrogen level is due to the different method of measurement, because the tray was only heated to 40 °C instead of 60 °C (like the other trays), a relatively much smaller gradient was observed. Although the measurement in itself is useful, it cannot be compared to the other trays, and therefore it is left out in the further analysis. The same trends observed below also hold for the 'only Gallium' tray. In figure 33, 34 and 35 below we plot the fits shown above together to find further trends emerging:

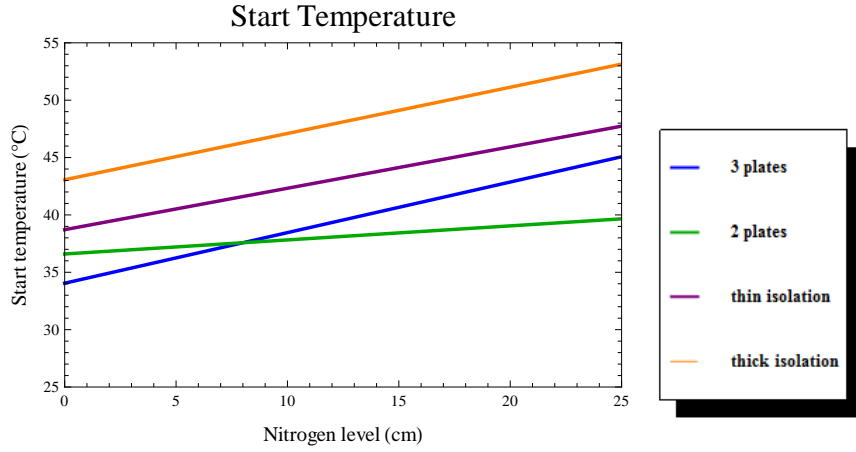


Figure 33: Fitted lines for start temperatures as a function of Nitrogen level. Layer weights (linearly translatable to thicknesses: 'thin isolation': 2.33 grams, 'three steel plates': 2.35 grams, 'thick isolation': 1.61 grams, 'two steel plates': 3.06 grams).

Figure 33 clearly shows that for increased Nitrogen levels the start-temperature, at which the crystal enters the camera view, increases. The slope of this dependence is almost identical for 'thick isolation', 'thin isolation', and 'three steel plates'. Two steel plates, which is a much thicker layer than the others, shows a much flatter slope as well as overall lower start-temperatures.



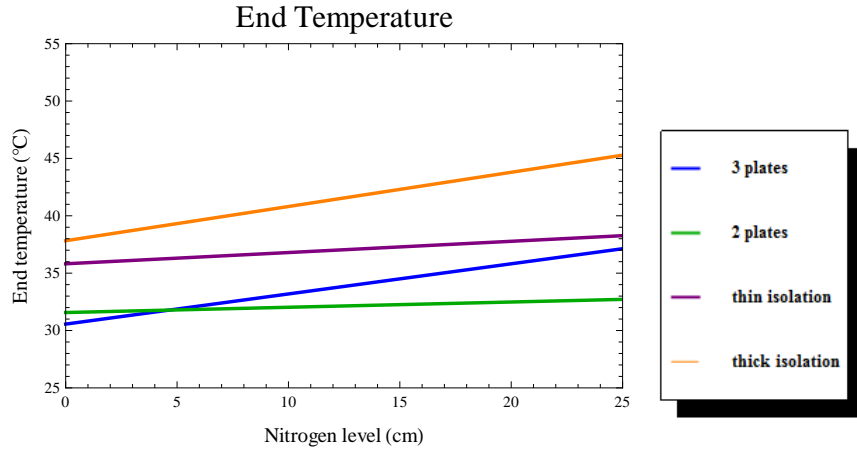


Figure 34: Fitted lines for end temperatures as a function of Nitrogen level. Layer weights (linearly translatable to thicknesses: 'thin isolation': 2.33 grams, 'three steel plates': 2.35 grams, 'thick isolation': 1.61 grams, 'two steel plates': 3.06 grams).

Figure 34 shows for all trays an increase in end-temperature for higher Nitrogen levels. What strikes is the resemblance of the slopes of respectively 'thick isolation' and 'three plates' and 'thin isolation' and '2 plates'. Although their absolute temperature levels differ, the slopes are nearly identical. It is presumed this is an effect of camera placement. The exact location of the camera view seems to have some influence on the end-temperature, even though this is less visible for the start-temperature.

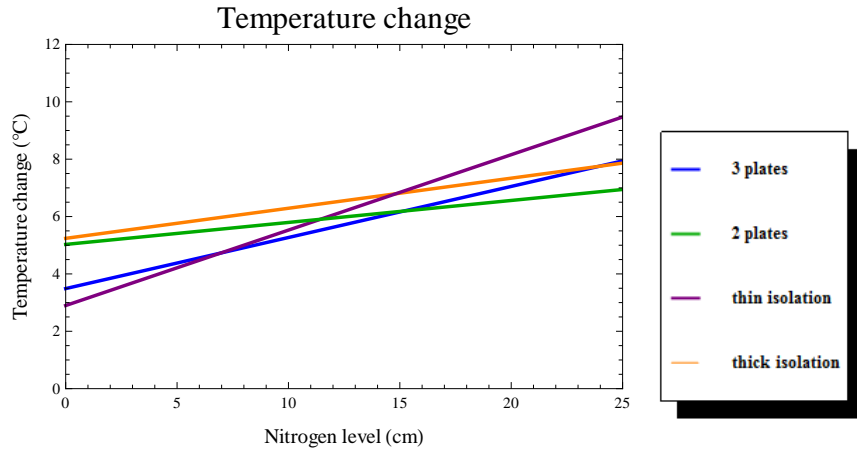


Figure 35: Fitted lines for temperature change as a function of Nitrogen level. Layer weights (linearly translatable to thicknesses: 'thin isolation': 2.33 grams, 'three steel plates': 2.35 grams, 'thick isolation': 1.61 grams, 'two steel plates': 3.06 grams).

Finally, figure 35 shows an increase in temperature change (defined as start-temperature minus end-temperature) for increasing Nitrogen levels. This relation is observed for all four trays. Although there is some difference between

the fits, it is not sufficiently large enough to draw any conclusions concerning the different characteristics of these trays to have had any influence.

#### **5.3.1 Conclusions from temperature gradient analysis**

As with the analysis of growth rate it is very hard to draw quantitative conclusions on differences between individual trays. However, for each individual sample tray, the trends are the same. For increasing Nitrogen level start-temperature, end-temperature, and temperature change all increase. This all indicates, using the arguments of section 4.3, that a higher Nitrogen level can increase the temperature gradient significantly. We will not draw any further conclusions concerning differences between trays, as the data shows too many irregularities.

## 5.4 Temperature gradients versus crystal growth rate

As further analysis for the three trays that were used for both growth rate measurements and the gradient analysis above, crystal growth rate and gradient measurements were combined. Temperature change was taken as a (as proven above in section 5.3) more direct measure for the magnitude of the temperature gradient across the tray, versus the crystal growth rate as determined by a fit of growth rate versus Nitrogen level from section 5.2.1. This resulted in figure 36.

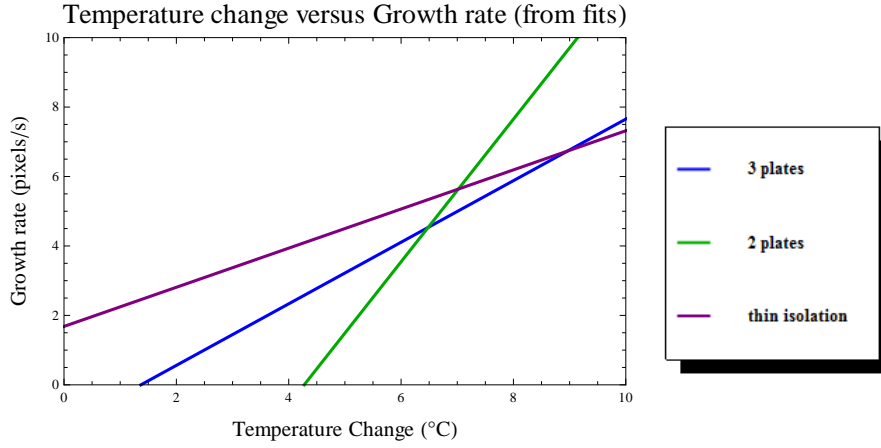


Figure 36: Crystal growth rate versus temperature change

The overall trend, visible in this graph, combines the two conclusions reached earlier:

- Crystal growth speed increases with increased Nitrogen level.
- The temperature gradient across the tray increases with Nitrogen level.

In one formulation this directly relates imposing a temperature gradient of a certain magnitude to the occurrence of certain crystal growth speed. Indirectly from the two conclusions above and directly from figure 36 it can be concluded that:

*Crystal growth speed increases with the magnitude of the temperature gradient across the Gallium layer.*

## 6 Discussion

Even though most results above have already been discussed in terms of their accuracy and conclusions that can or cannot be drawn from them, it is still worthwhile to emphasize some issues regarding the results of this research project.

### 6.1 Undercooling

As already mentioned, the initial aim of this research was to try and create a setup in which Gallium could be undercooled to temperatures significantly below its freezing temperature. This could not be realized for a few reasons: The cooling mechanism with the copper rod was too slow to quickly dissipate heat, the tray and Gallium cooled down very slowly. In itself, this meant crystals had a lot of time to form at the melting temperature.

Another factor was the tray itself: manual fiddling caused scratches and bumps in the tray. The Gallium layer was not always applied perfectly, sometimes resulting in a layer that was not completely smooth, or not fully connected to the razor. These imperfections meant crystals could start growing from nucleation sites (see section 2.1.1) earlier than if the tray and Gallium layer would have been completely flat.

It was observed a few times that a newly inserted Gallium layer ('only Gallium' as in figure 17) could be cooled to at least 12 °C without nucleation and growth of crystals. Crystallization then only started by inserting a pipette (small mechanical shocks didn't work). The pipette often distorted the flat layer, and the resulting crystallization would pop through the surface of the Gallium at random points. One time, when the pipette was intentionally inserted near the razor, a crystal front shot across the tray very quickly. This measurement however, could not be repeated by heating the sample to 60 °C and cooling it again, crystallization would start at higher temperatures again ( $\approx 35^\circ\text{C}$ ). We expect this has to do with small crystals remaining on the razor, even when the other side of the tray is 40 °C above the melting point of Gallium.

Because of the low repeatability, the decision was made to not pursue this crystallization any further here. Nevertheless, the observations clearly indicate a severe undercooling and fast crystal growth can be achieved.

### 6.2 The tray-razorblade-heating plate-construction

Although the experimental setup in its full form serves its purpose of crystallizing and measuring Gallium crystal growth, it was made with just a vague idea of what would be an effective design. Now quite some experience modifying and measuring with the device has been attained, quite a few modifications to improve performance and accuracy can be proposed.

- The tray should be permanently attached to the razor, with the razor being the back end of the tray and not, as it is now with one-third of the tray being useless heat-sink. This may create a smoother surface inside the tray, creating less angles on which a crystal could start growing, giving more chance of reaching an undercooled state.
- The connection between razor and liquid Nitrogen could be isolated a lot better using permanently attached flexible isolation. The connection rod

could also be made a lot thicker, in order to decrease thermal resistivity.

- The tray could be made with thinner edges without risk of breaking it. This would reduce the heat capacity of the tray.
- A better system to test layers should be designed. This could possibly be done with different more shallow trays, maybe using small insertable plates that exactly fit the compartment (this was not the case with the steel plates available).
- The Matlab script that was written sometimes had trouble distinguishing the crystal fronts. When accuracy is improved, we may also see a distinction that could not always be made now. The FWHM of some growth rate histograms was quite large sometimes. This could either be noise, or a growth rate slowly changing in time.
- Although an easy solution is not known, a recurring problem plaguing the setup was that after three hours of measurements a thick layer of ice ( $\approx 0.5\text{cm}$  or even more) would have formed on the razor, sometimes obscuring the camera view.

### 6.3 Thermocouples

One fairly easy improvement would be attaching a thermocouple close to the razor, to measure temperature there. An even better way of studying temperature gradients would of course be to somehow measure temperature everywhere in the tray. Related to the temperature measurements an accurate way of determining what part of the tray is in the camera view would also be needed, otherwise the absolute temperature readings would still be meaningless.

## 7 Conclusions

The first conclusions from this research may seem trivial, but since this was a first explorative research project in this direction, it was unknown if some more basic things could be realized. Therefore, they deserve to be mentioned:

- It is possible to freeze Gallium in a controlled fashion, inducing crystal growth from a desired position or side.
- It is however not possible to induce undercooling in a Gallium layer with this setup.
- There is optical contrast between solid and liquid Gallium.
- Gallium crystal growth rates could be determined using a camera and computer image processing. The Gallium crystal growth rates were measured were found to be in the range of 2 to 7 pixels/s, which corresponds to 13  $\mu\text{m/s}$  to 44  $\mu\text{m/s}$ .
- Even though aluminium is in principle protected against Gallium embrittlement because of a natural oxide layer, scratching and temperature changes will cause the Gallium to reach the atomic aluminium, heavily corroding sample trays.
- Objects made from stainless steel, such as the new tray and razor blade are impervious to this embrittlement.

With the final experimental setup several measurements were performed, from which the following conclusions can be drawn:

From the measurements in section 5.2.1 it can be concluded that

- Gallium crystal growth rate increases by approximately 3 pixels/s (equivalent to 19  $\mu\text{m/s}$  when Nitrogen level increases from 5 cm to 20 cm.

Since the temperature gradient across the tray increases with Nitrogen level, as shown in section 5.3 we can conclude that:

- An increased temperature gradient across the length of the Gallium layer increases the crystal growth rate of Gallium. (section 5.4).

## 8 Recommendations for further research

Of several small side-experiments (i.e. extremely thin layers, crystal angle measurements, high undercooling), it was already said why they were not pursued any further. Nevertheless, they are still interesting subjects, that could probably be researched with some more effort specifically driven towards solving the issues experienced during this project. A measurement of the crystal lattice orientation of Gallium crystals in a solid sample could be done using elektron microscopy. In particular employing Orientation Imaging Microscopy, where Kikuchi Backscatter Patterns are recorded in order to determine locally the crystal orientation.

The preparation of very thin layers could be done by using a process like spin-coating or using an a tray with an extremely shallow Gallium compartment. Of both these subjects, however, it is doubtful if the knowledge it would yield is worth the effort.

### 8.1 Achieving higher undercooling

We feel the most important and interesting follow-up research could be done in the direction of achieving the original goal of this research project, as formulated in subsection 2.1.4.

The original goal was designing a setup that could prepare a gallium layer in an undercooled state (i.e. in the liquid phase below its freezing temperature), and measure crystal growth speeds.

Measuring crystal growth speeds is already possible. With the knowledge we have now about building this setup, it should be possible to build a setup that can cool our Gallium even quicker. Several ideas for this have already been described in section 6.2.

However his is not enough, because for the gallium layer to reach an undercooled state no crystals should present in the liquid before cooling (see section 2.1.1). Therefore the setup should ideally be built so that the *whole tray including the razor*, can be heated to temperatures above the melting temperature (say approximately  $60^{\circ}\text{C}$ ). Then it should be cooled down quickly, for instance by pushing two razorblades together, one razor attached to the cooled copper rod, and one razor inserted in the tray.

The most difficult challenge would be to design a mechanism to induce crystallization once a certain amount of undercooling is reached. This mechanism should do the same every time to ensure crystal growth is not dependent on the manner of crystal growth activation. This could probably be done by lowering a needle on an arm into the Gallium layer, next to the razor.

Since we have already observed this undercooling a few times, we feel that with the considerations above it should be possible to design a setup to repeatedly induce and record actual undercooled Gallium crystal growth.

## 9 Acknowledgements

Firstly, I would like to thank Prof. Bart Kooi for his supervision during this research project. Also many thanks to Ing. Gert ten Brink, who helped me a lot over the weeks with all problems, difficulties and challenges to do with designing a new measurement setup. I would also like to thank Msc. Gert Eising for his help with the custom camera-software, as well as the heating plate control system and the matlab crystal growth script. Finally, my thanks to the rest of the NMI-group, without them this research project would not have been as fun as it was now.



## 10 References

### References

- [1] <http://en.wikipedia.org/wiki/Gallium>
- [2] <http://en.wikipedia.org/wiki/Copper>
- [3] <http://en.wikipedia.org/wiki/Nitrogen>
- [4] Kittel, Introduction to Solid State physics, third Edition, John Wiley and Sons Inc. Chapters 1 and 2 about crystal lattices.
- [5] Harrie van den Akker/Rob Mudde, Fysische transportverschijnselen (physical transport phenomena), third edition, VSSD. Chapter three is about heat transport and steady-state versus on-steady state.
- [6] <http://www.webelements.com/gallium/crystal-structure.html>, a website listing properties of all elements in the periodic table.
- [7] D.A. Porter, K.E. Easterling, Phase transformations in metals and alloys, Van Nostrand Reinhold company, 1981 first edition.

## A Custom Matlab code

The code below is the main script, which loads the images to be analyzed, and performs edge detection. The further analysis is done by other scripts already available in the NMI-group.

```
function [ outputcluster , images ] = TimeImageAvgP( directory , filter ,
startindex , lastindex , avgfile , skip , differenceimage , tmname , gmname , histname )

%[S1] = TimeImageAvgP('E:\bachelorproject\Measurements\rvsbakje3\7cm3\ ', '*7cm3*
%directory folder , filters only files with correct name, start and stop
%number of file , file to average all others with , to correct for nonuniform
%lighting , skips in steps of skip , galliumfilter subtracts 2 images to
%filter , diffimage specifies how much further an image is selected for this
%subtraction .

%SPEEDIMAGE Summary of this function goes here
% Detailed explanation goes here
list = dir([directory filter]);

wholelist = list(startindex:lastindex); %list with all frames , because gallium
list = list(startindex:skip:lastindex); %list with all frames to be analyzed

%load file , filter it , determine border
timeimage = zeros(1024,1024);
fractions = zeros(1,length(list));
times = zeros(1,length(list));
levels = zeros(1,length(list));
zerotime = -1;
%avgimg = imread([directory '\ ' avgfile]);
%smoothfilt = fspecial('average');
%avg = imfilter(avgimg(1:1024,1:1024,1), smoothfilt);

for i=1:1:length(list)-differenceimage-1

    time = GetTimeFromPath([directory '\ ' list(i).name]);
    if zerotime < 0
        zerotime = time - 1;
    end

    img1 = imread([directory '\ ' list(i).name]) ;
    red = double(img1(1:1024,1:1024,1));

    img2 = imread([directory '\ ' list(i+round(differenceimage/skip)).name]) ;
    %red2 = double(img2(1:1024,1:1024,1)) - double(avg);
```

```

[ size_x size_y ] = size(red);
levels(i) = FindThreshold2(red);

img1filt=medfilt2(rgb2gray(img1-img2),[15 15]);

img1edge=medfilt2(edge(img1filt,'sobel','nothinning'),[8 8]);

border=img1edge;

for x=1:size_x%1024
    for y=1:size_y%1024
        if border(x,y) == 1
            %if timeimage(x,y) == 0 %only new borders
            timeimage(x,y) = time-zero_time;
            %end
        end
    end
end
%fractions(i) = sum(sum(red>levels(i)))/(1024*1024);
times(i) = time;

fprintf(' %d ', i);
end
fprintf(' \n ');

% growthrate
[growthrate gx gy] = GrowthRate(timeimage, 16);

%histogram
histogram=GrowthRateHist(growthrate, histname);

outputcluster = struct('fr',fractions,'ti', times, 'tm',timeimage, 'gm',growthrate);
e1=figure(2);imshow(outputcluster.tm);caxis([0 1e5]);title(tmname);
e2=figure(3);imshow(outputcluster.gm);caxis([0 12e-3]);title(gmname);

saveas(e1,tmname,'png');
saveas(e1,tmname,'fig');
saveas(e2,gmname,'png'); saveas(e2,gmname,'fig');

end

```